ISSN 2347-3487

Effect of Synthesis methods on the Properties of Magnetic Material

Farwa Mushtaq[1], M. Anis-ur-Rehman[2], A. Haq[1]
[1]Physics Department, G.C. S/Town, Rawalpindi, Pakistan
[2]Applied Thermal Physics Laboratory (ATPL), Department of Physics,
COMSATS Institute of Information Technology, Islamabad 44000, Pakistan

Abstract

$Ba_{1-x}Pb_xFe_{12}O_{19}$ composition (x=0.0 to 1.0) synthesized by Co-precipitation and Sol-Gel methods. In Co-precipitation method $BaCO_3$, PbO and Fe $(NO_3)_3$.$9H_2O$ were used as basic ingredients. Acids and Di-H_2O were used as solvents. Molar ratio of cations was 12. pH of solution kept constant at 13. All samples sintered at 965±5^oC for three hours. Lead own properties, synthesis at room temperature and substitution in R-block of structure were the reasons for decrease of phase purity from "x" =0.0 to 70% for "x"=1.0. Decrease in phase purity and heterogeneity of material caused the properties to decrease. In Sol gel method, Nitrates (salts) and Ethylene glycol (liquid) were the basic material used. The mixed solutions dried out on a hot plate whose temperature was maintained constant at 200±2^oC. Pellets formed by applying suitable hydraulic pressure and then sintered at same temperature written above i.e. 965±5^oC for three hours. 100% phase purity achieved. All properties modified. Temperature and frequency dependent electrical properties investigated and reported here. DC and AC obtained properties were useful for different electronics and computer devices like capacitors, smart storage devices and multilayer chip inductors. Overall, both these properties improved through sol-gel method as compared to co-precipitation method. It was because of improvement in phase purity and change in morphology of synthesized material.

Key words

Co-precipitation; Sol-gel; Lead dopant; Preference occupancy; Phase purity; Electrical properties improved; smart applcations.

Council for Innovative Research
Peer Review Research Publishing System
Journal: JOURNAL OF ADVANCES IN PHYSICS
Vol. 10, No. 1
www.cirjap.com, japeditor@gmail.com

ISSN 2347-3487

Introduction

Ferrites being magnetic material are very important for today's scientific and technological development. Its classification depends upon composition and structure, which differentiate its applications. Hexagonal ferrite itself is a big family and also known as hard ferrite. U, W, X, Y, Z and M are its family members[1]. M-type is very much attractive for researchers, advancement of technology and for device fabrications. It is because of easy availability of raw materials, easy to synthesize and its excellent chemical, corrosion stability and durability[2, 3].

M-type family possesses complex structure and consists of SRS^*R^* blocks. For Ba hexaferrite formation, Ba^{2+}, Fe^{3+} and O^{2-} involve. The reactant mixture must self-assemble into S and R blocks or structures at their own suitable temperature and time. The reactions conditions that favor the formation of γ-Fe_2O_3 and Fe_3O_4 during synthesis would also encourage barium ferrite formation. Thus reaction kinetics of these compounds along with other components shown can be seen in M-type structure [4].

In order to improve the properties of M-type materials particularly Ba-hexaferrite, researchers have used and applied different methodologies and techniques. In these techniques first attempt was to optimize the synthesis parameters and obtain purity (Phase) especially when substitutions introduced. The physical properties of dopant like ionic radii, site preference, its mobility, valance ability are important. Better control on synthesis parameters improves the phase purity and morphology, which on other hand improves the properties. Above methods and applied techniques decide the structural and morphological growth of material as a result purity and properties improved. In all synthesis methods reaction kinetics provide environment for respective elements (ions) to use energy for their movements and occupy their respective crystallographic position in the structure then minimize. This mechanism is the crystal growth process, hence particular crystal structure – phase completes. Properties of any material are strongly affected by the cations distributions, microstructure developed and phase obtained [5-7].

In presented paper, comparison of two synthesis methods with respect to phase purity, microstructure and their morphology has discussed. Change in these factors changes the properties. $Ba_{1-x}Pb_xFe_{12}O_{19}$ (x=0.0 to 1.0) composition was synthesized by co-precipitation and sol-gel method. The comparative analysis of the obtained results has presented here. Both are low temperature synthesis methods, low cost, easy to manage and almost uniform cations distributions are the main advantages of these methods[8].

1- Experimental Procedure

In co-precipitation method, $BaCO_3$, Fe $(NO_3)_3.9H_2O$ and PbO were used as basic ingredients. Barium carbonate dissolved in (con.)HNO_3 while PbO in (con.) HCl. NaOH used as precipitating agent. Cations molar ratio of iron to barium used was 12. Solid Fe $(NO_3)_3.9H_2O$ and NaOH were dissolved in Di-H_2O. All these ingredients were stochiometrically calculated, weighed and then used. Three independent solutions formed were mixed together at room temperature. For ferrite precipitation, molar solution (M=5) of NaOH was added into it. About 97% NaOH solution was added at once while the remaining used to acquire pH=13 at the end. The obtained solutions were stirred for half an hour. It was necessary for uniform distribution of cations, minimization of impurity and better homogeneity. This was co-precipitation synthesis and completed at room temperature. For identification of samples these solution were given name as A_o (x=0.0), A_1 (x= 0.2), A_2 (x= 0.4), A_3 (x= 0.6), A_4 (x= 0.8) and A_5 (x= 1.0).

All solutions were washed with de-ionized water along with vigorous stirring so that impurity minimized and homogenization improved. After washing, paste like material placed in an oven at 110±2°C for overnight. The dry material obtained transformed into powder form. The obtained powder then converted into pellets by applying suitable hydraulic pressure of 1000 lbs. /$inch^2$ for five minutes. The dry pellets then sintered in a furnace for three hours at 965±5°C. These sintered pellets were used for different characterizations.

In order to synthesize the same composition with sol-gel method, the basic precursors used were nitrates of barium, lead, iron and ethylene glycol. Stochiometrically calculated materials then dissolved and magnetically stirred in 200ml ethylene glycol solution whose quantity was also optimized. These mixed solutions (from 0.0 to 1.0) were stirred and heated on a hot plate whose temperature was maintained constant at 200±2°C. Because of heating liquid contents started to evaporate, then gel like material formed. At the end, it burnt and dried material obtained.

In sol-gel method, vigorous stirring and heating the liquid media helps the different metallic components to mix quickly at atomic level. This mixing mechanism provides an opportunity especially in terms of energy for different ions to move, occupy their respective positions and then minimize their energies in phase as a result purity improves[9]. Then pellets formed by applying suitable hydraulic pressure of 1000 lbs/$inch^2$ for five minutes, same pressure as used in co-precipitation method. The dried pellets then placed in a furnace at 965±5°C for three hours. $Ba_{1-x}Pb_xFe_{12}O_{19}$ synthesized was ready for different characterizations.

Comparing both synthesis methods, sol gel looked better and easy than co-precipitation method. It is very useful for industrial production. Sol-gel was easy to manage because no extra parameters like molar ratio, molarities, pH and washing were required. To differentiate it from others samples these were given name as AA_o, AA_1, AA_2, AA_3, AA_4 and AA_5 for Pb=0.0, 0.2, 0.4, 0.6, 0.8 and 1.0 respectively. All chemicals used were analytical graded. They were from sigma Aldrich, Mäurk and Fluka. They were 99.99 % pure.

ISSN 2347-3487

2-Structural Analysis

Since both compositions have same nature with only difference in synthesis methodology and the techniques applied. Sintering temperature and time was same. All characterizations tools were same and measurements recorded and noted under same conditions and procedures.

2.1- XRD Analysis

Samples synthesized with co-precipitation and Sol-gel methods were scanned for five minutes from 2θ = 0 up to 80^{o} and 70^{o} respectively by using CuK_{α} radiation source. Wavelength available and used was 1.5406Å.

By comparing both indexed XRD graphs (figure 1.1 and figure 1.3) it was noted that in co-precipitation method, impurity phases started to develop as the lead dopant introduced and it continued to increase up to end. In Sol-gel graph, No such phase(s) was detected or seen by XRD machine. Its reason was simple that in co-precipitation synthesization was at room temperature while in sol-gel method synthesization completed at 200±2°C. At room temperature different reactions unable to complete, stresses and distortions due to lead substitution in place of barium initiated impurity phases like $PbFe_2O_{2.67}$, $Ba_3Fe_{26}O_{41}$ and $PbFe_2O_4$ developed. Stresses and distortions were generated due to greater ionic radii (Pb^{2+} = 1.76Å) than smaller ionic radii (Ba^{2+} = 1.37Å) [10]. Other reasons were low melt point of Pb (950°C) and fast

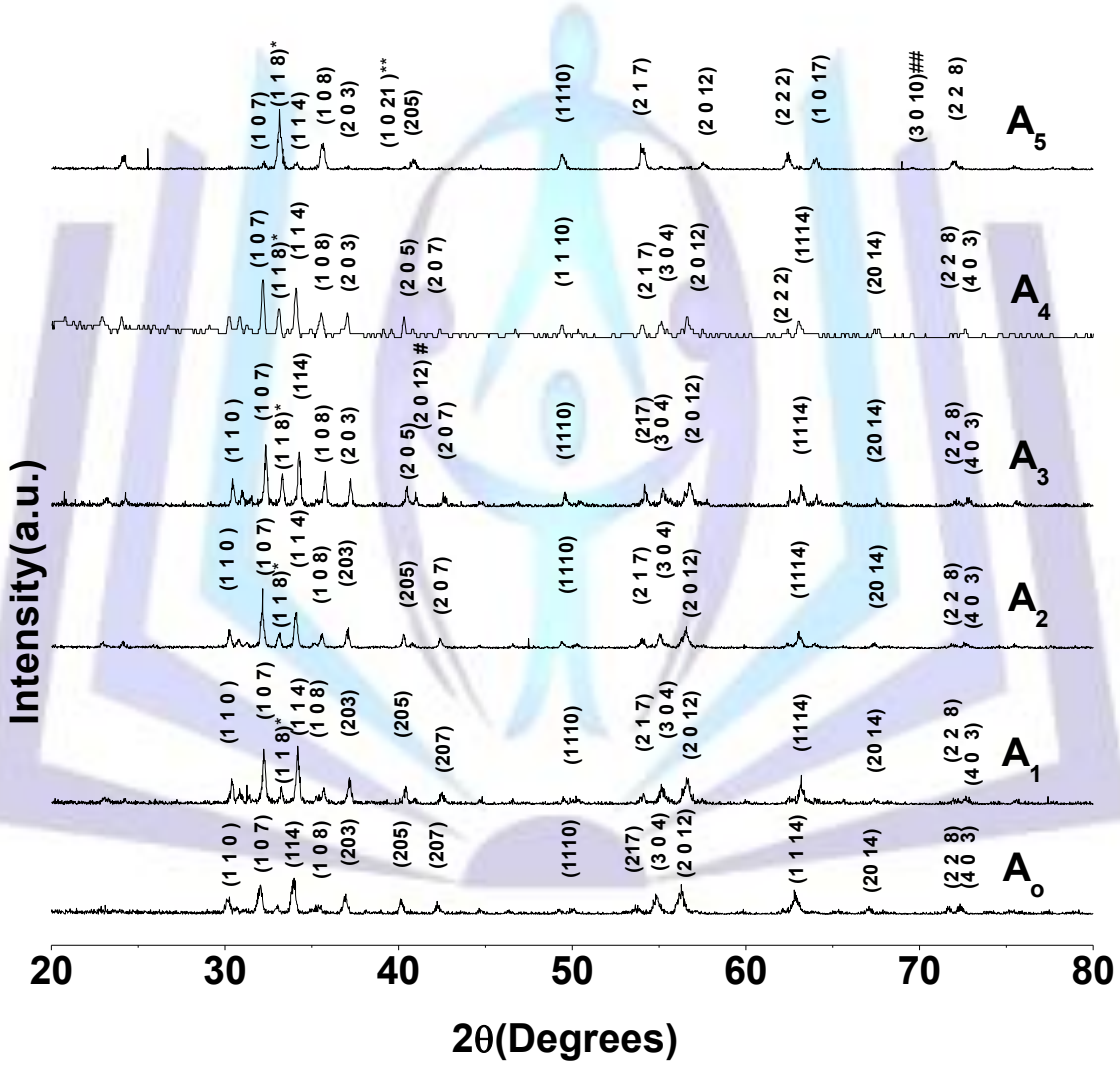

Figure 1.1:- Indexed XRD pattern of $Ba_{1-x}Pb_xFe_{12}O_{19}$ synthesized by Co-precipitation method.

mobility than Ba . Impurity phases are * $Ba_3Fe_{26}O_{41}$, ** $PbFe_2O_4$, # $PbFe_4O_{17}$, # # $PbFeO_{2.67}$. Fast mobility of Pb^{2+} ions than Ba^{2+} caused the crystallization process to enhance. All these factors increased the impurity phases. As a result, phase purity decreased from 100% for "x"= 0.0 to 70% for "x"=1.0. It has shown in figure 1.2. However phase purity achieved was better than already reported with same method [7, 9, 10].

ISSN 2347-3487

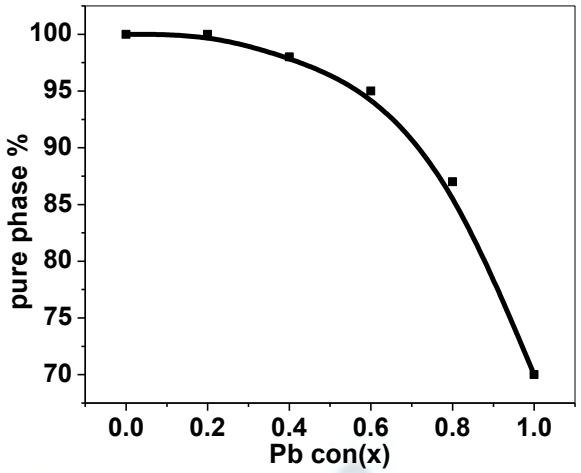

Figure:-1.2 Purity - Decreased in co-precipitation method.

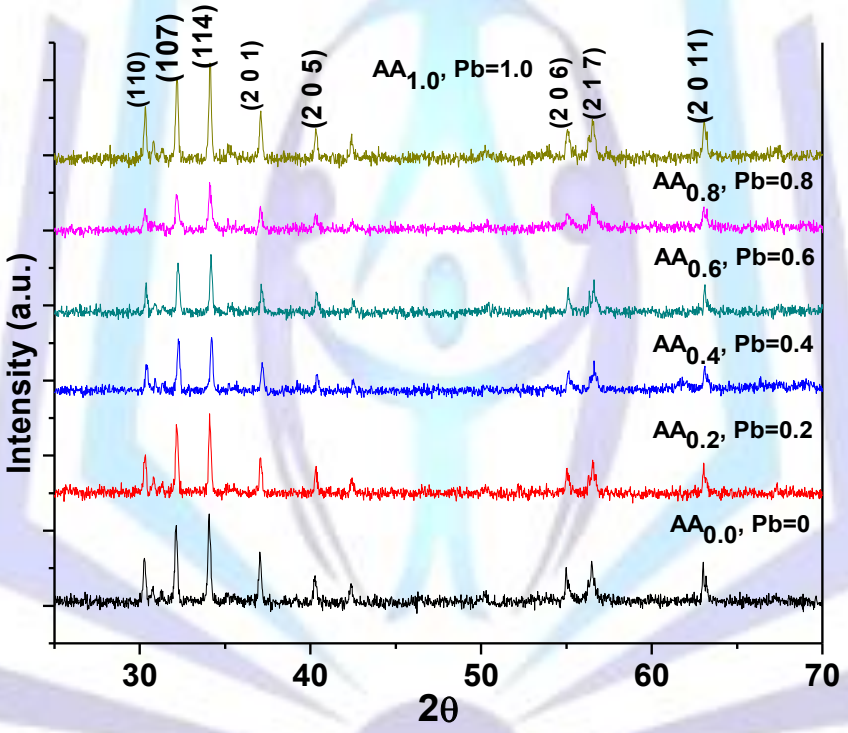

Figure1.3:- Indexed XRD pattern of $Ba_{1-x}Pb_xFe_{12}O_{19}$ - Sol gel method

In case of sol-gel, ingradients and techniques applied changed. Heating was the key factor which differentiates it from co-precipitation so results improved. Heating factor was the basic requirement in sol-gel method. It provided the required energy which along with small energy of stresses and distortions enough for individual ions/atoms to move and occupy respective positions inside the structure. When structure completed energy started to minimize in phase so chances of initiating impurity phases also minimized. It was possible because of strict control on applied conditions like stirring and time.Indexed XRD did not detect any impurity peak(s) as shown in indexed graph of figure 1.3. These peaks were matched with JCPD cards. These cards were 00-084-0757, 00-027-1029 for $AA_{1.0}$ i.e. for $PbFe_{12}O_{19}$. For other compositions, these cards were 00-041-1373 and 00-017-0660.

Comparing both indexed XRD graphs of same composition showed that reactions kinetics and energy minimization were almost in phase in sol-gel. It was not possible in co-precipitation method because those samples were prepared at room temperature. Heating was the key differentiating factor because completion of different reactions and starting of S and R blocks in SRS*R* structure were different particularly when there was 180^o rotation in this structure [11, 12]. Hence, structurally transformation from Ba-hexaferrite to Pb-hexaferrite obtained.

2.2- Complete Transformation

By comparing both XRD indexed patterns of $Ba_{1-x}Pb_xFe_{12}O_{19}$ (x=0.0 to 1.0) produced different results in terms of phase purity and characterizations. XRD machine did not detect/indicate any impurity phase in Sol-gel indexed patterns while same machine showed impurity peaks in case of co-precipitation. In these compositions Pb was going to replace Ba in R-blocks of compound. By applying modified and optimized synthesized techniques purity improved. In co-precipitation method, purity achieved was 70% better than already reported with same method [7]. Through sol-gel almost 100% purity obtained, so complete transformation from $BaFe_{12}O_{19}$ to $PbFe_{12}O_{19}$ was obtained and reported.

2.3 - Lead Preference Occupancy

It has reported by Thongmee et al [13] that all dopants have their own preference occupancy sites. In present study, Pb^{2+} ions being greater ionic radii have preference occupancy site, i.e. octahedral (12k, 2a and 2b) of the hexagonal structure which is slightly larger than tetrahedral ($4f_1$ and $4f_2$) [14, 15]. In $Ba_{1-x}Pb_xFe_{12}O_{19}$ (x=0.0 to 1.0) composition, Ba occupies different occupancy sites in R and R^* blocks. Physical properties of dopant like ionic radii, low melting point and higher mobility than Ba^{2+} ions were also important beside site preference (see figure 4.1). Up to certain value of "x" dopant chances to occupy its preference site become maxima after that it may go to any other sites like tetrahedral or any other. These movements or distortions were responsible of creating abrupt change in phase development and properties of end material [16-18].

2.4- Structural growth analysis

Beside fast crystallization process, synthesis methodology and physical properties of lead were important to decide the variations in different structural parameters**.** In co-precipitation method, synthesis was at room temperature while continuous heating was a key factor in sol-gel synthesization i.e. 200±2°C. Structural variations observed in both methods which played its role in defining properties.

It has reported in the literature [19, 20] that Pb^{2+} ions being volatile nature and higher mobility helped to move randomly in different directions. As a result, grain growth has different behavior in both methods. In case of sol-gel, induction of lead dopant initially helped the growth mechanism to modifiy while in co-precipitation grain growth increased initially. So lead as dopant played different role in grain growth mechanism. Being volatile nature dopant has chance to go S-block. Its diffusion at boundaries of R and S also have different role in both methods. So valtile and mobility itself affected the growth mechanism in both methods. Different graphs below explain and support this trend. SEM micrographs also explained and supported this growth mechanism.

2.5- Crystallite size

It has reported [7, 21] that oxides dopant like PbO, Al_2O_3 and SiO_2 etc. are responsible of non- uniform trend in crystallite size "*D* ". In co-precipitation method lead substitution up to "x"= 0.6 increased "*D*" from 38nm to 59nm. Heat generated in small area due to presence of sufficient quantity of dopant in that small area collectively helped the crystallite size to grow or enhance. Beyond "x"=0.6 this trend changed. Increased quantity of volatile dopant now moved freely in different areas like R and S blocks(may be) so quantity now in large areas restricted the growth (59 to 33nm) however it modified the dimensional growth as shown by SEM micrographs (figure 3.1). In case of Sol-gel heat of 200±2°C temperature and heat of dopant stresses and distortions combined. This combined energy moved or travelled randomly in different directions so not enough energy to increase "*D*". In other words energy there moved to such sites like voids or dislocation areas diffused/ absorbed there that caused "*D*" to reduce from 47nm to 23nm . However when dopant concentration increased beyond "x"=0.6 combined energy was sufficient to enhance the crystallite size (23nm to 58nm). Scherer's formula was applied to calculate it. Small variation in "*D*" is because of volatile nature and mobility of dopant ions.

In case of co-precipitation method, "*D*" increased up to "x"=0.6 beyond this value same type trend observed in Sol-gel and it decreased from "x"=0.6 to 1.0 (co-precipitation) while it decreased form "x"=0.0 to 0.6 for sol-gel method. Such trend for oxides dopant has also reported in literature [7]. Dopant being volatile in nature may go to or pile up on those sites /positions where it unable to play role of enhancing the grain growth. This mechanism changed when dopant occupancy change its occupancy state inside the structure thus grain growth changed. Obtained crystallite size lies within 50nm range in both methods is useful for magnetic recording media applications [22-24].

Because of higher density of lead (11.34 g/cm^3) than barium (3.51g/cm^3), properties affected at large. This higher value was responsible of increase of X-ray density (ρ_x) and bulk density (ρ_m) in both synthesis methods. In case of co-precipitation method it increased from (5.27 g/cm^3 to 5.48 g/cm^3) and bulk/ mass density from (2.22 g/cm^3 to 4. 17 g/cm^3).

ISSN 2347-3487

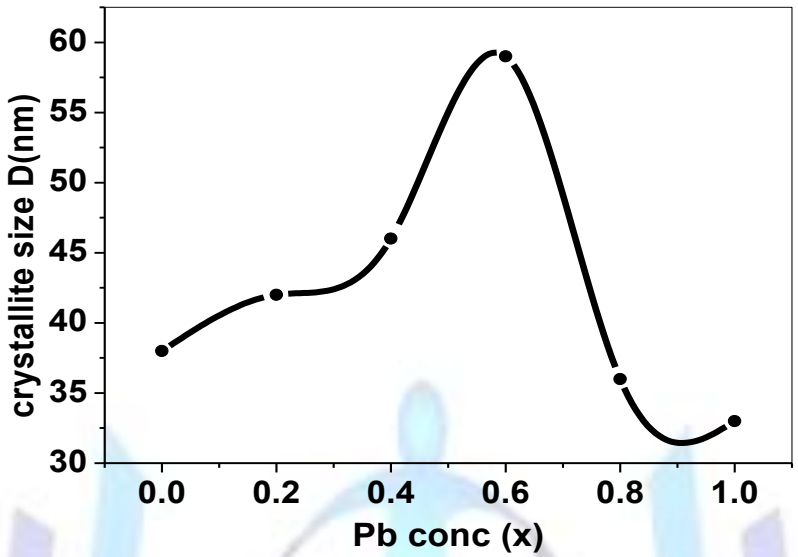

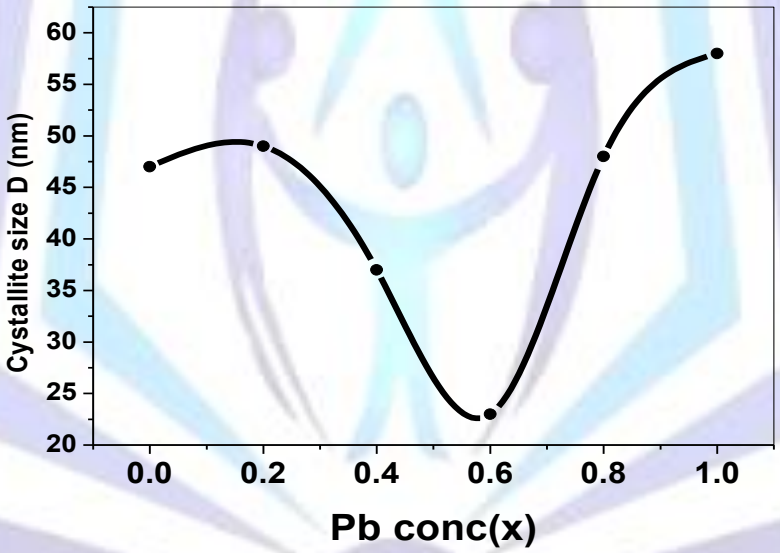

Figure 2.1:- Crystallite size Co-precipitation (above) Sol-gel (below)

2.6- Lattice parameters and Volume

Because of volatile nature and higher ionic radii of dopant, all structural parameters varied. Physical properties of dopant was forced to move and diffuse /occupy in different sites / directions or occupancy sites[25] in non-uniform quantity. It was possible because dopant was going to replace Ba^{2+} ions in R and R^{*} blocks of structure (180°). Dopant also has different affect at boundaries of S an R blocks. All these factors caused the lattice parameters "*a*" and "*c*" to vary. Stresses and distortions were the other important parameters to have an effective role as reported by Teh and Jefferson[26]. This change in lattice parameters was also responsible of change in size of unit cell. Similar phenomena was also observed and reported by Mingquan Liu et al.[27].

In co-precipitation method lattice parameter "*a*" reduced more (5.92Å to 5.82Å) than in sol-gel (5.91Å to 5.89Å), while "*c*" modified itself. It was important for defining different properties particularly magnetic properties. Here again smart variation in sol-gel than co-precipitation noted. Following graphs of lattice parameters and volume are explaining this whole mechanism in much detail.

ISSN 2347-3487

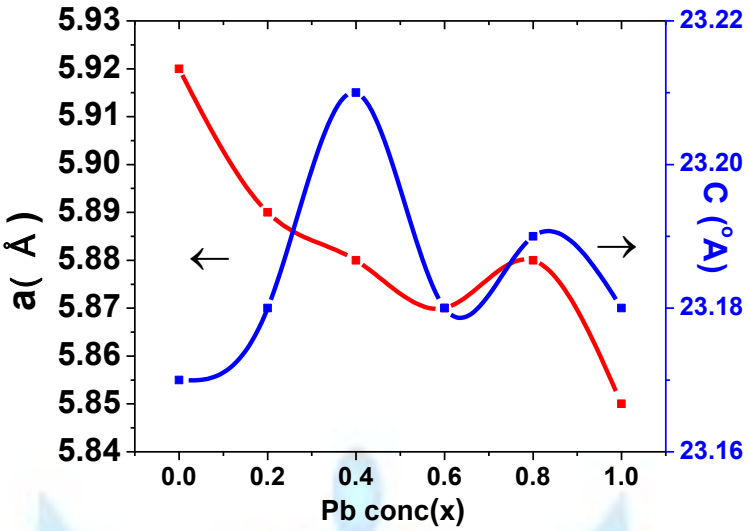

Figure 2.2:- Lattice parameters for co-precipitation method

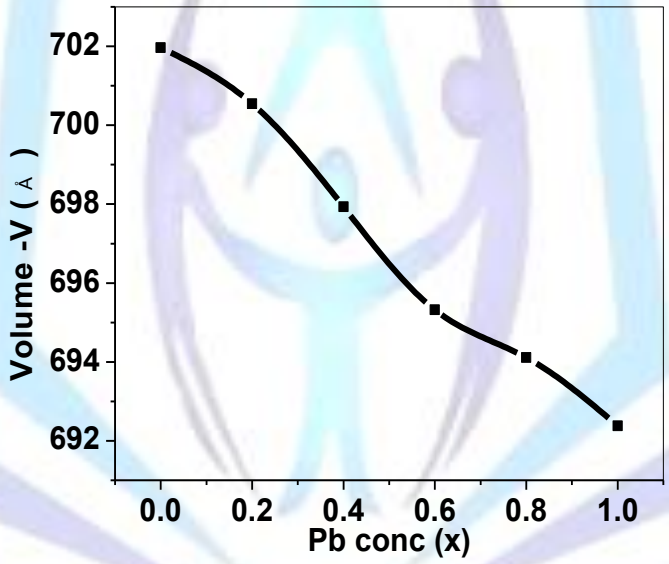

Figure 2.3:- Reduction in volume with increase of Pb^{2+} concentration-Sol-gel

Comparing both synthesis methodologies it observed that because of lead own different properties like change in preference occupancy and volatile status lattice parameters modified itself as a result reduction in volume of unit cell was observed. This factor has made the mass transportation slow within particles during crystal growth process. It makes grains small i.e. grains growth enhanced mechanism restricted as discussed [7]. This phenomenon supports from the crystallite size graphs (Figure 2.1). This makes structure compact as confirmed by reduction in porosity. Porosity reduced from 58% $AA_{0.0}$ to 25% $AA_{1.0}$ (Sol-gel) and from 46% - A_0 to 15% -A_5(Co-precipitation).

3- SEM Analysis

To analyze the surface morphology and dimensional growth of composition synthesized by two different low temperature methods SEM was used. Both samples sintered at same temperature for three hours. XRD graphs showed that 70% and 100% phase purity achieved. Lead substitution not only enhanced crystallization process but also modified the dimensional growth. Both micrographs below have clearly differentiated this phenomenon. Best hexagonal structures seen in the co-precipitation samples. From sample A_0 to A_4 hexagonal structure reshaped itself because of increase of lead contents. But growth restricted in next concentrations. At the same time, different morphological and dimensional growth observed in sol-gel. Sharp edge and platelets like structures in co-precipitation as compared to petal and paper like structures in sol-gel. This morphology played an important role in analyzing different properties.

ISSN 2347-3487

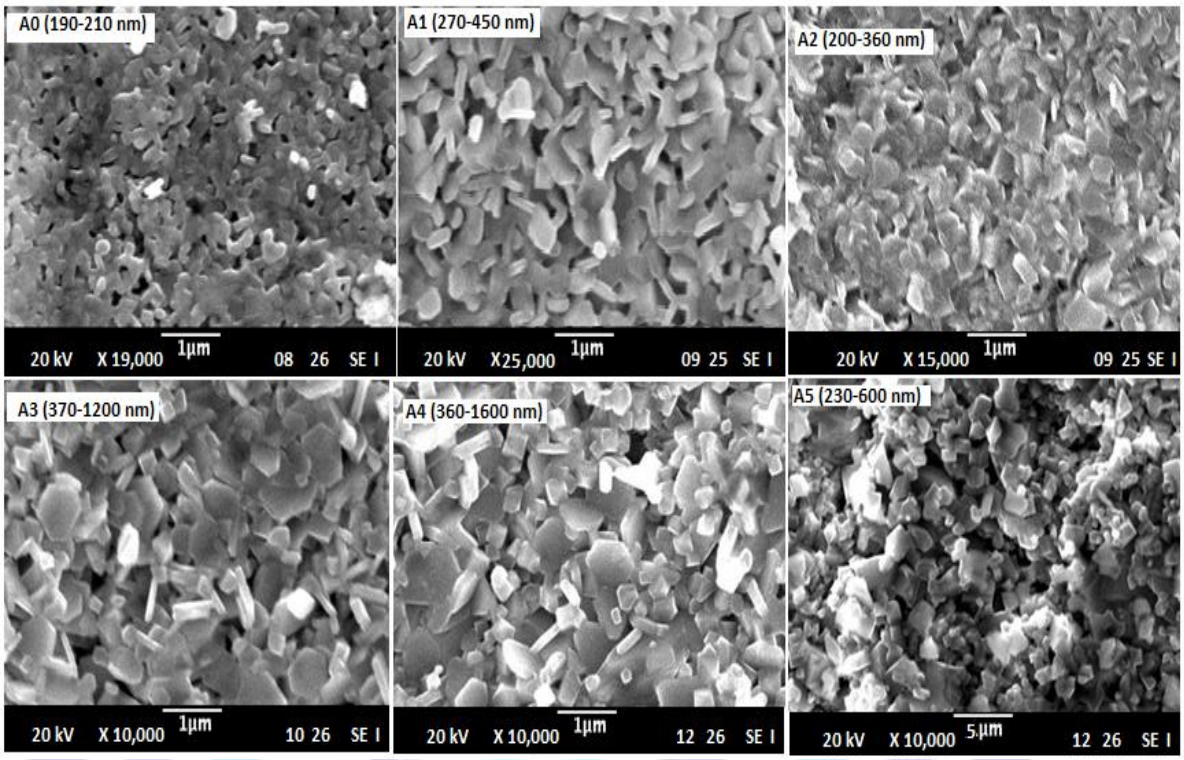

Figure 3.1:- SEM micrographs of $Ba_{1-x}Pb_xFe_{12}O_{19}$ synthesized by Co-precipitation method.

Particle size estimated and their distributions are useful for magnetic recording media applications[24]. Pb dopant has increased (*c*) and decreased (*a*) which helped above growth transformation. Platelets like structures are very important in defining magnetic properties.

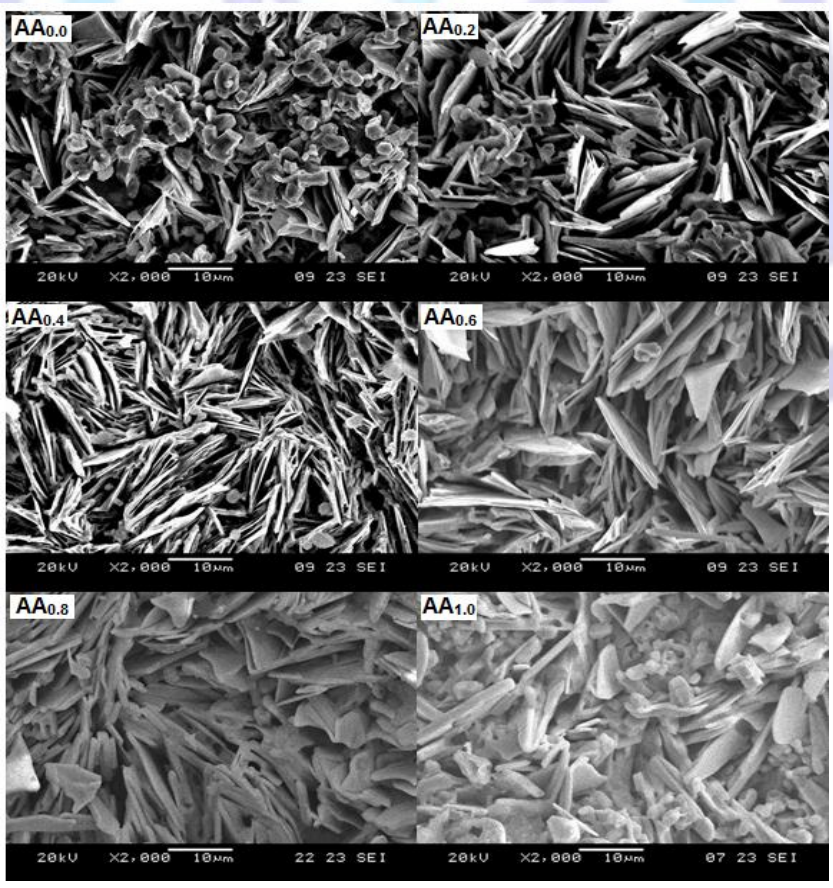

Figure 3.2:- SEM micrographs of $Ba_{1-x}Pb_xFe_{12}O_{19}$ synthesized by Sol-gel

ISSN 2347-3487

4-Electrical Characterizations

Temperature dependent dc and frequency dependent ac properties were investigated for $Ba_{1-x}Pb_xFe_{12}O_{19}$ are reported here. Because of obtained phase purity and variation in structural parameters and morphology, it was important to study these characterizations. Before going to discuss and explain the electrical properties of doped compositions, Figure 4.1 shown below has explained the octahedral and tetrahedral sites of the complex hexagonal structure[28]. These sites are important to analyze these properties. In all ferrites, conduction and polarization phenomenon are because of generation of Fe^{2+} ions due to oxidation of Fe^{3+} ions on octahedral and tetrahedral sites[29, 30].

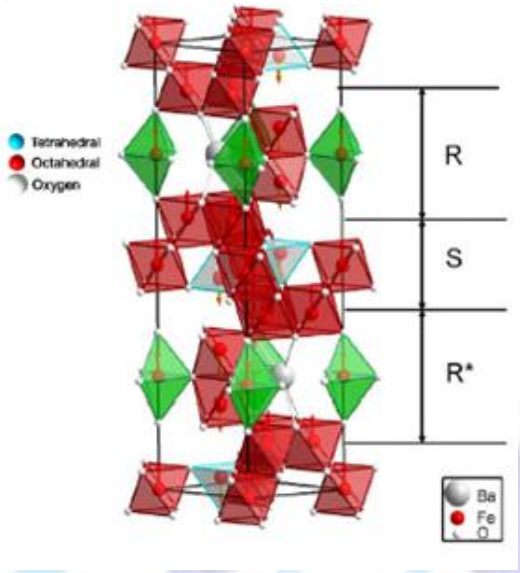

Figure 4.1:- Complex hexagonal structure representing tetrahedral and octahedral sites in M-type Ba-hexaferrite [28]

4.1- DC Properties

Temperature dependent dc properties were investigated by two-probe method because ferrites are high resistive materials. In order to analyze different dc parameters, dc current (I_{dc}) was measured as a function of temperature from 300K to 733K for all samples for co-precipitation method. For sol-gel, (I_{dc}) was measured from 328K to 748K. Parameters like resistivity (ρ), activation energy (ΔE), mobility (μ_d) and charge carrier concentration (n) were measured and calculated. The doping effect with respect to its concentration, site preference or occupancy studied and reported.

4.1.1- Resistivity, Mobility and Activation Energy

As discussed in literatures[31, 32] that Fe^{3+} ions in M-type ferrites occupy octahedral and tetrahedral sites i.e. 12k, 2a , 2b all have spin in one direction (up) while two tetrahedral sites $4f_1$ and $4f_2$ have spin opposite (down). The resistivity of material (ferrites) depends upon Fe^{2+} ions on octahedral sites, this site is slightly larger than tetrahedral sites [31, 33, 34] . Graph of Figure 4.2 (a) and Figure 4.2(b) showed that resistivity of Pb doped composition has increased with increase in Pb^{2+} concentration.

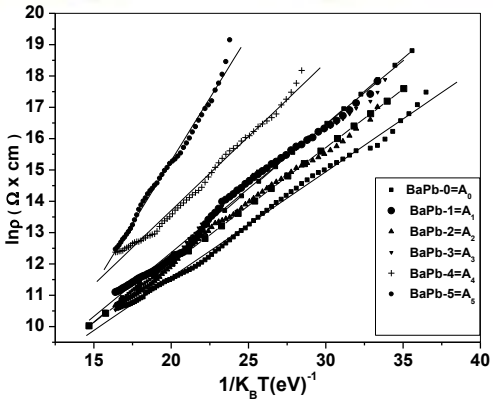

Figure 4.2 (a):- Arrhenius plot for dc resistivity [co-precipitation]

ISSN 2347-3487

According to Verwey hopping model change in charge carrier concentration with change in temperature influenced the hopping or jumping of charge carriers from one octahedral site to next[35] i.e. conduction. It is also affected by doping concentration, phase purity, heterogeneity and morphology of synthesized material.

Variations in the graphs of figure 4.2 (a and b) showed that factors like substitution in R-block, occupancy, variation in "x", phase purity, change in amount of grain boundaries and their morphology played different role in both methods. Variations of these parameters in Sol-gel method were small because of phase purity and almost same grains dimensions. All these factors have different role in samples of co-precipitation method.

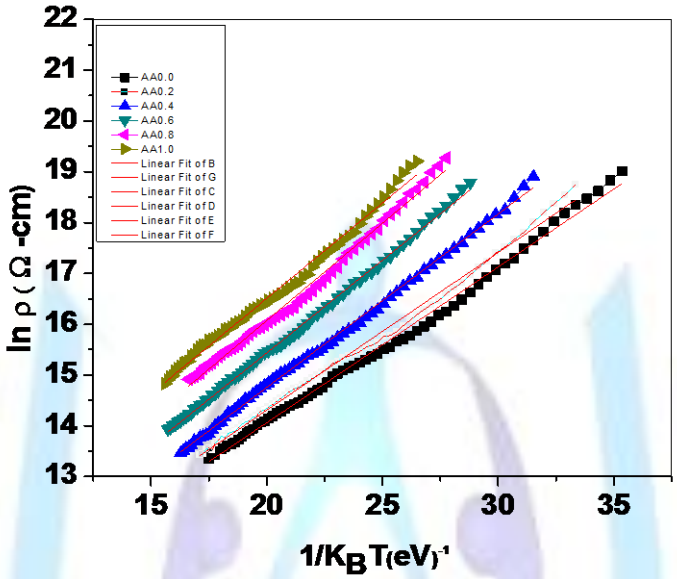

Figure 4.2(b):- Arrhenius plot for dc resistivity for $Ba_{1-x}Pb_xFe_{12}O_{19}$ [sol gel].

Graphs below showed almost increasing behavior/trend for different parameters. Resistivity increased because being higher ionic radii and non- magnetic dopant (Pb^{2+} ions) occupied octahedral sites. This occupancy made difficult for Fe^{2+} ions to generate and hope. Other factors like voids, impurity phases, dislocations, heterogeneity played their role in restricting conduction mechanism. All these parameters act as energy barriers for conduction mechanism so it decreased. Lead dopant affected different dc parameters has explained below.

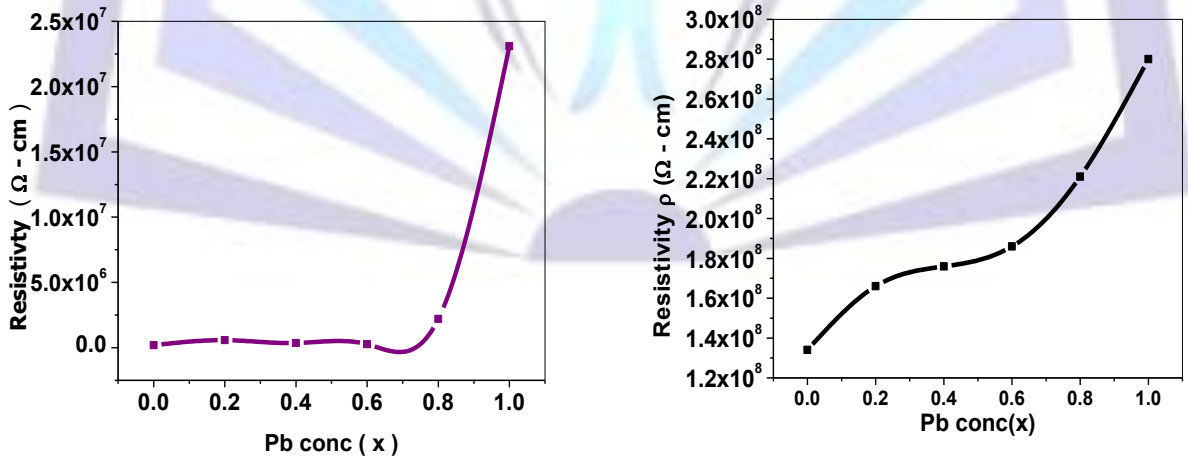

Co-precipitation method Sol-gel method

4.3:- Trend of resistivity as a function of Pb conc(x) for co-precipitation and sol-gel method

Increasing trend in resistivity looked more smooth and prominent in sol-gel than co-precipitation method. Movement of Pb^{2+} ions within structure formed different pockets or zones or blocks that provided trapping centers for hopping charges. Because of these centers and change in grain boundaries energy required for hopping charge also increased [36]. In ferrites, charge carriers acquired energy to come out from trapping center and to hopping.

ISSN 2347-3487

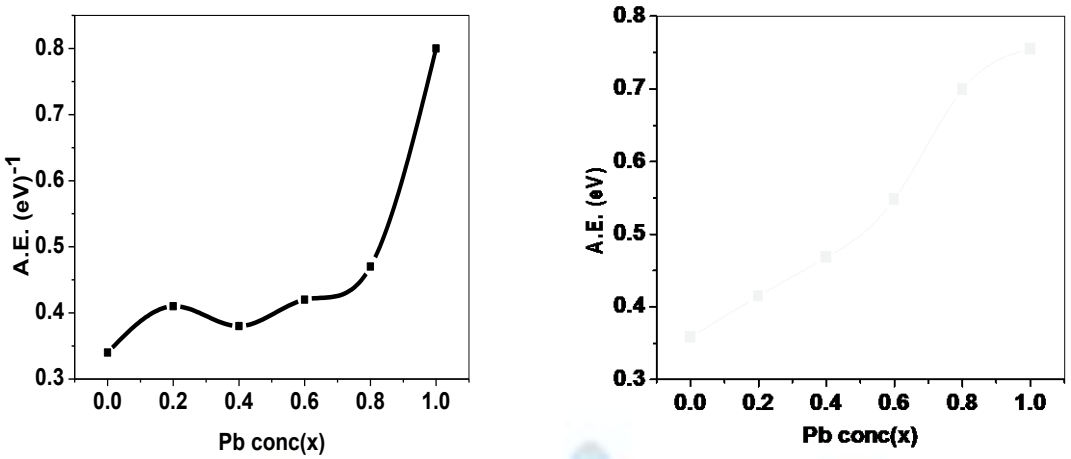

Co-precipitation Sol-gel

4.4:- Activation energy (A.E.) as a function of Pb conc(x).

Researcher has given name activation energy to that energy. Increase in resistivity confirmed by increase of activation energy as shown above. Energy increased in both cases confirmed that Pb^{2+} ion substitution was responsible of increase of energy and resistivity. Researchers have given name to this phenomenon as a result of many body problems[37]. Different factors discussed above were responsible of decrease of mobility. It has also proved by relation (μ_d = *1/neρ*). Following two graphs are explaining the variation in mobility because of dislocations. Mobility of lead ions itself was non-uniform inside the structure. Increase in mobility mean that some quantity of Pb^{2+} ions has gone to tetrahedral sites or some of Fe^{2+} ions were forced to migrate from tetrahedral to octahedral site which resulted in increase of mobility from "x=0.2 to 0.6[38]. In other words here conduction increased. From above discussion, it has confirmed that lead substitution is responsible of variations of resistivity in co-precipitation more than sol-gel. It has reported by Kligner [39] that if activation energy is greater than 0.4eV than it is polaron hopping , less than this will electron hopping. In present discussion polaron hopping is prominent than electron hopping.

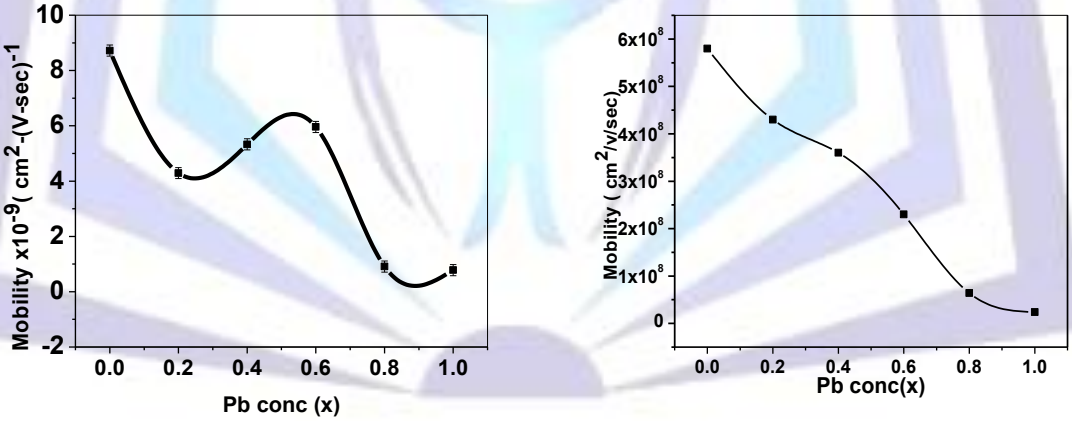

Coprecipitation Sol-gel

4.5:- Mobility (μ_d) as a function of Pb conc(x).Coppt and Sol-gel .

5- AC Characterizations

Fast development of communication technology generated another kind of environmental pollution (i.e. radiation hazards). It is associated with electromagnetic interfacing (EMI) and electromagnetic compatibility (EMC). Higher dielectric and magnetic loss are the prime parameters to address these unwanted signals. This can be achieved by selecting suitable dopant in suitable quantity and sintering temperature[40]. In studied composition, lead used to modify the dielectric properties thus suitable for above application to some extent. Low losses are also acceptable for other type of applications. In present compositions, capacitance (*C*) and dissipation factor (*D)* were measured as a function of frequency by using 6440B Winker Frequency Precision Analyzer. Measurements were made from 20Hz to 3MHz. Appropriate formulas were used to calculate dielectric constant (*ε*) and dielectric loss (*tanδ*).

ISSN 2347-3487

5.1- Dielectric constant

Figure 5.1 showed that dielectric constant decreased with increase of applied frequency or electric field in our studied compositions, a normal behavior of all ferrites. According to Maxwell –Wagner model ferrites consist of conducting grains and non-conducting grain boundaries (two layers model). The prepared composition $Ba_{1-x}Pb_xFe_{12}O_{19}$ possesses heterogonous structure. The electron exchange between $Fe^{2+} + Fe^{3+} \leftrightarrow Fe^{3+} + Fe^{2+}$ was the deciding factor for the magnitude of dielectric constant and dielectric loss[40]. Dielectric constant and loss in ferrites depend upon space charge polarization and charge formation at the grain boundaries. Temperature, dopant and dipole strength played an effective role in dielectric properties of studied compositions.

Pb^{2+} substitution developed non-uniform variation in polarization process as shown by graphs. Synthesized compositions consist of heterogeneous elements of different valances which have coordination of different strength with each other and with oxygen [41]. Lead substitution, impurity phases, dislocations, voids and change of morphology when interacted with electric field of varying strength, polarization mechanism affected strongly. Variation in dopant concentration was another factor which affected the generation and hopping of Fe^{2+} ions on octahedral sites thus magnitude of Fe^{3+}/Fe^{2+} ions concentration also disturbed and changed within composition. All these phenomenas were responsible of variation in dielectric constant in irregular form. Graphs of figure 5.1 have explained that variations is more prominent in co-precipitation than in sol-gel because of above discussed factors. Some electrons during hopping may fall or trapped by grain boundaries and potential wells given name correlated state as reported [42] so polarization decay trend becomes slow thus decreases. It has shown in graphs. Heterogeneity of composition, phase purity and grains modification or morphology affectively made this decaying trend to vary in non-uniform way. At some applied frequency points, it mixeed to each other. Mixing trend is almost same and different in co-precipitation samples than sol-gel like A_o and $AA_{o.o}$. High resistivity also discouraged the polarization and conductivity mechanisms[40].

Graphs also indicated that exchange phenomenon ($Fe^{3+} \leftrightarrow Fe^{2+}$) did not follow the frequency of applied field [43]. Like A_2 sample behavior decreased in the middle and increased from both ends while it responded slowly to the applied field [44, 45]. So large number of Fe^{2+} ions if hopped, polarization increased as a result dielectric constant and dielectric loss increased [40, 46].

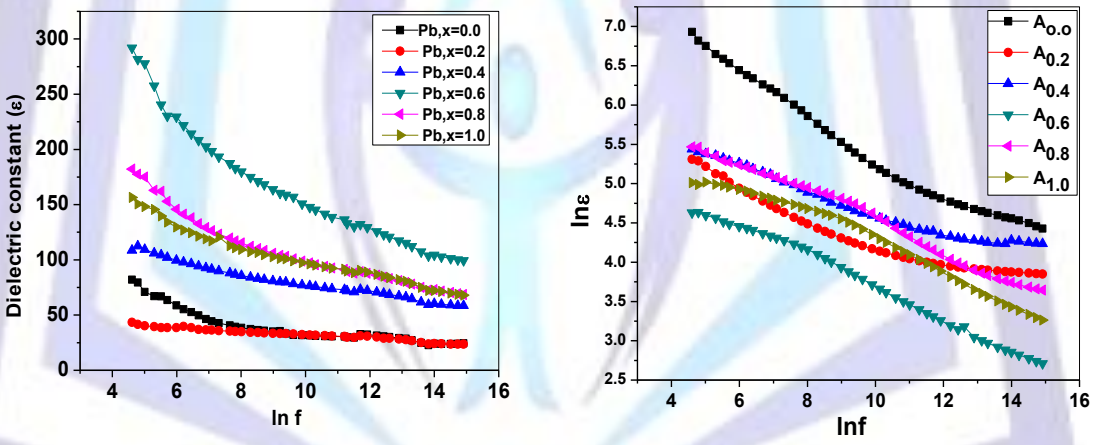

Fig 5.1:- Variation in dielectric constant (*ε*) as a function of frequency *(lnf)*.

5.2- Dielectric loss tangent

It is the dissipation of energy denoted by 'Q'. Dielectric loss (*tanδ*) occurs in dielectric materials due to following process[47].

1- Charge defects dipoles.

2- Electron hopping

Dipoles formed in ferrites due to change in magnitude of cation states (Fe^{3+}/Fe^{2+}) by applied electric field. Substitution of lead in place of barium was another effective parameter to change this magnitude. This response changed with change of applied frequency. At low frequency dielectric loss was because of electron hopping and at high frequency it was because of polaron hopping[47]. It was noted that for A_1 (x= 0.2; tanδ= 0.12 and 0.6), A_4 (x= 0.8; tanδ = 0.36 and 0.16), at 200kHz and 3MHz respectively as compared to un-doped composition A_o (x=0.0; tanδ = 0.31 and 0.16).

Dielectric loss slightly increased at higher frequency in case of A_2, A_3 and A_5. It was because of increased concentration of Pb^{2+} ions, non-uniform and hindrance in hopping and due to rapid movements of Pb^{2+} ions on different crystallographic sites of structure. Because of these factors impurity increased so loss increased. Low loss are useful for high frequency applications while higher loss is useful to control the environmental pollution[34].

ISSN 2347-3487

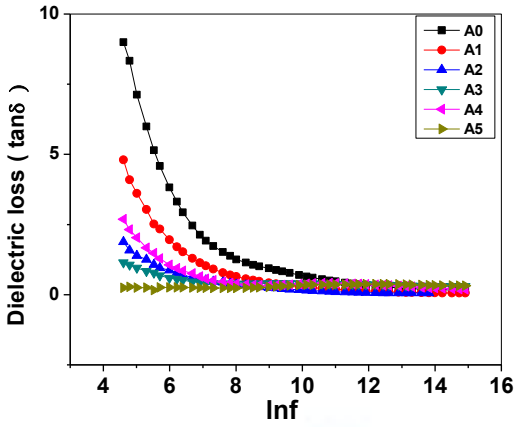

Figure 5.2:- Dielectric loss (tan δ) for $Ba_{1-x}Pb_xFe_{12}O_{19}$ as function of frequency (co-precipitation method).

Dielectric loss for same composition as a function of frequency has presented in the graph below for sol-gel method. It showed different trend as compared to co-precipitation method. Dielectric loss has increased for the sample $AA_{0.0}$ and $AA_{0.2}$ rapidly than others. It was because of occurrence correlated states in these samples[37]. Heterogeneity of material, higher mobility of lead ions and coordination of Fe^{3+} ions with O^{2-} form dipole of different strength in different directions/orientations. These Dipoles and dislocations within structures provided trapping centers for hopping charges. Those trapped charges when interact with applied electric field of varying strength they developed their own oscillations of different strength, researchers have given name relaxation frequency [48]. The electron hopping between $Fe^{2+} \leftrightarrow Fe^{3+}$ ions produces another relaxation frequency. These different kinds of relaxation frequencies (also called characteristics of resonance peaks) when associated with space charge polarization phenomenon altogether showed the behavior given name correlated state as shown in above graphs[49]. Dielectric loss rises in such regions.

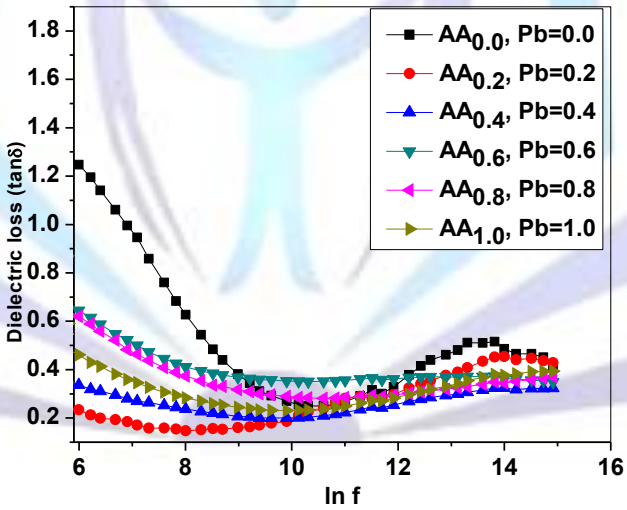

Fig. 5.3:- Dielectric loss (tan δ) for $Ba_{1-x}Pb_xFe_{12}O_{19}$ as function of frequency (Sol-gel).

The dielectric loss increased in case for 0.0 and 0.2 doping in the frequency range (starting 40 kHz, maximum at 800 kHz and minimum at 3 MHz). In case of $AA_{0.2}$ or 0.2 doping (starts rise at 5 kHz , max at 100 kHz and reduced to minimum at 3MHz). At high frequency, grain dimensions, their morphology and heterogeneity helped the hopping charges to pile up at grain boundaries. Their response to applied frequency was very different in the regions of correlated states. Because of these different mechanisms, chances of resonance phenomenon reduced /diminished. It has shown in the graph.

As the prepared material possesses magnetic properties so motion of these peaks was because of motion of domain walls also [50]. Increase in loss is useful parameter for minimizing environmental pollution due to electromagnetic Interference (EMI)[34] .

6-Conclusions

$Ba_{1-x}Pb_xFe_{12}O_{19}$ with x=0.0 to 1.0 was synthesized by co-precipitation and sol-gel methods. Both compositions were sintered in a furnace for three hours at 965±5°C. Structural and electrical (ac and dc) characterizations were investigated and comparatively discussed here. Composition synthesized with co-precipitation method was at room temperature. It produced excellent hexagonal structure, their distribution but phase purity dropped i.e. 70%. But it was better than already reported with same synthesis method. Same composition when synthesized with sol-gel, phase purity was almost 100% with excellent morphology. Because of improvement in phase - purity and morphology magnetic and electrical properties improved than co-precipitation. Sol gel synthesis method used here must be useful for industrial production of this material. The physical properties of lead like dopant –higher ionic radii unable to produce impurity in sol-gel because of its heating at 200±2°C. Particle size estimated, high resistivity and dielectric constant obtained were useful for different components of electronics and computer industries like recording media applications, storage devices like capacitors and other appliances where high resistivity is required. High dielectric loss obtained is useful against today's communication radiation hazards.

Acknowledgment

Thanks to National Research Program for Universities (NRPU) and Higher Education Commission, Pakistan for financial support. Bundles of thanks to Applied Thermal Physics Laboratory (ATPL), CIIT, Islamabad for unlimited excess for technical supports. Thanks to a man provided me unconditional support for SEM and magnetic analysis of samples.

References

1. Albanese. Recent advances in hexaferrite ferrites by the use of nuclear spectroscopic methods. De Physique Tome. 38(4) (1977) Cl-85 - C81-95.

2. G. Albanese , B.E. Watts , Diaz-Castanon. Magnetic and Mössbauer investigation of PbFe12–xGaxO19 hexagonal ferrites. J. Mat. Sci. 37 (2002) 3759-3763.

3. M. Iqbal , M. Naeem. Physical and electrical properties of Zr–Cu substituted strontium hexaferrite nanoparticles synthesized by co-precipitation method. J. Chem. Engg. 136 (2008) 383-389.

4. Y. Liu, H.B. Zhang, J.D. Duan, Y. Gao, L.L Wang, Y. Li. Magnetic properties of Mn/Co/Sn substituted barium hexaferrites synthesized by an improved Co-precipitation method. J. Adv. Mat. Res. 239-242 (2011) 3052-3055.

5. S. Singhal, A.N. Garg, K. Chandra. Evolution of the magnetic properties during the thermal treatment of nanosize BaMFe11O19 (M=Fe, Co, Ni and Al) obtained through aerosol route. J. Mag. Mag. Mat. 285 (2005) 193-198.

6. C. Sudakar, G.N. Subbanna, T.R.N. Kutty. Hexaferrite–FeCo nanocomposite particles and their electrical and magnetic properties at high frequencies. J. Appl. Phy. 94(9) (2003) 6030.

7. M. Liu, X. Shen, F. Song, J. X. Meng. Microstructure and magnetic properties of electrospun one-dimensional Al3+substituted SrFe12O19 nanofibers. J. S. S. Chm. 184(4) 2011871-876.

8. S. Nasir, Muhammad Anis, M. A. Malik. Structral and dielectric properties of Cr doped Ni-Zn nano ferrites. J. Phys. Scr. (2010) 83.

9. X. H. Zhang, Q. Ling, Z. hiyuan. Kinetics and magnetic properties of sol–gel derived NiZn ferrite–SiO2 composites. J. Mat. Letts. 57(20) (2003) 3031-3036.

10. G. Hadjipanayis. Nanophase hard magnets. J. Mag. Mag. Mat. 200 (1999) 373-391.

11. A. Sharbatia, S.C.A. Ghasemib, I. alAmric, C.F. C. Machadod, A. Paesano JRd. Synthesis and magnetic properties of nanocrystalline Ba3Co(0.8-x) Mn 0.4 Ni2x Fe24 O41 prepared by Citrate Sol-Gel Method. Digest. J. NanoBiostr. 6 (1) (2011) 187 - 198

12. M.A. Ahmed, N. Okasha, R.M. Kershi. Dramatic effect of rare earth ion on the electrical and magnetic properties of W-type barium hexaferrites. Physica B. J. Con. Matter. 405(16) (2010) 3223-3233.

13. S. Thongmeea P. Winotaib , I. M. Tangc Boron site preference in B-doped barium hexaferrite. Research Areticle J. Sci. Asia. 29 (2003) 51-55.

14. C. Singh SBN, I. S. Hundiara, K. Sudeendran*, K. C. J. Raju*, K. N. Rozanov. Microwave and electrical properties of Co–Ti substituted Ba–Sr ferrite. J. Cerm. – Silikáty 54 (2) 2010 116-121.

15. M. N Ashiq, M. J. Iqbal, Hussain, I. Gul. Effect of Al–Cr doping on the structural, magnetic and dielectric properties of strontium hexaferrite nanomaterials. J. Mag. Mag. Mat. 323(3-4) (2011) 259-263.

16. Y. Liu, M.G.B. Drew, J. Wang, M. Zhang, Y. Liu. Efficiency and purity control in the preparation of pure and/or aluminum-doped barium ferrites by hydrothermal methods using ferrous ions as reactants. J. Mag. Mag. Mat. 322(3) 2010 366-374.

17. M. Toulemonde, Ch. Dufour, A. Meftah, E. Paumier, F . Studer. Track creation in SiO2 and BaFe12O19 by swift heavy ions: a thermal spike description. Nuclear Instruments and Methods. J. Phy. Res. B 116 (1996) 37- 42.

18. K. K Mallick, P. Shepherd, R. J. Green. Magnetic properties of cobalt substituted M-type barium hexaferrite prepared by co-precipitation. J. Mag. Mag. Mat. , 312(2) (2007) 418-429.

19. S. Diaz-Castanon a , B.E. Wattsb , R. Yapp b, PbFe12O19 thin films prepared by pulsed laser deposition on Si/SiO2 substrates. J. Mag. Mag. Mat. 220 (2000) 79-84.

20. P. C. Dorseya, K. S. Grabowski, D. L. Knies, P. Lubitz, D. B. Chrisey, J. S. Horwitz. Epitaxial Pb–Fe–O film with large planar magnetic anisotropy on (0001) sapphire. J. App. Phy. Lett. 70(9) (1997) 1173-1176.

21. J. Kreise1 H. Vincent,1 Raman spectra and vibrational analysis of BaFe12O19 hexagonal ferrite. J. S. S. Chem. 137(1998) 127 - 137.

22. C.G Stefanita. Slides of magnetism - From Bulk to Nano. Book - Springer Series. J. Mat. Sci. (2008) 1-188.

23. J.L. Sinclair Temperature and orientation effects on the magnetic properties of doped barium ferrite thin films. J. IEEE Tran. Mag. 30(6) (1994) 4050-4052.

24. T. Fujiwara. Barium Ferrite media for perpendicular recording (invited). J. IEEE Trans. Mag. 21(5) (1985) 1480-1485.

25. B. Kaur, M. Bhat, F. Licci, R. Kumar, S.D. Kulkarni, P.A. Joy, K. K. Bamzai, P.N. Kotru. Modifications in magnetic anisotropy of M—type strontium hexaferrite crystals by swift heavy ion irradiation. J. Mag. Mag. Mat. 305(2) (2006) 392-402.

26. G.B. Teh, D.A. Jefferson. High-Resolution Transmission Electron Microscopy studies of Sol–Gel derived cobalt-substituted barium ferrite. J. S. S. Chem. 167(1) (2002) 254-257.

27. Mingquan Liu, Shen X, Song F, Xiang J, Meng X: Microstructure and magnetic properties of electrospun one-dimensional Al3+substituted SrFe12O19 nanofibers. J. S. S. Chem. 184(4) 2011 871-876.

28. V.Harris, C. Anton, et al Recent advances in processing and applications of microwave ferrites. J. Mag. Mag. Mat. 321(14) (2009) 2035-2047.

29. M. J. Iqbal, M.N. Akhtar. Physical and electrical properties of Zr–Cu substituted strontium hexaferrite nanoparticles synthesized by co-precipitation method. J. Chem. Engg. 136 (2008) 383-389.

30. N. Karen, M.N. Akhtar, I. Tkachov. Millimeter-Wave Magnetooptics: New Method for characterization of ferrites in the millimeter-wave range. J. IEEE Tran. Micro Thr. Tecnq. 47(6) (1999) 2636-2344.

31. D.B. Lisjak, B. Vladimir, M. Drofenik. The influence of microstructure on the microwave absorption of Co–U hexaferrites. J. Mag. Mag. Mat. 310(2, Part 3) (2007) 2558-2560.

32. C. Singh, I.S. Hundiara, K. Sudheerndran, K.C. J. Raju. Microwave and electrical properties of Co-Ti substituted Ba-Sr ferrites. J. Cer. Int. 54(2) 2010 116-121.

33. D. Lisjak Drofenik M: The low-temperature formation of barium hexaferrites. J. Eur. Cerm. Soc. 26(16) (2006) 3681-3686.

34. C. Singh, I.S. Hundiara, K. Sudheerndran, K.C. J. Raju. Microwave and electrical properties of Co-Ti substituted Ba-Sr ferrites. J. Ceramics – Silikáty. 54(2) (2010) 116-121.

35. G. Asghar, Anis ur Rehman. Variation in structural and dielectric properties of co-precipitated nanoparticles strontium ferrites due to value of pH. J. Allys Comp. 509(2) (2011) 435-439.

36. A. Vermaa, T.C. Goela , M.I. Alamb. Dielectric properties of NiZn ferrites prepared by the citrate precursor method. J. Mat. Sci. Engg. B(60) (1999) 156-162.

37. S.E. Shirsath, S.S. Jadhav, B.G. Toksha, S.M. Patange, K.M. Jadhav. Remarkable influence of Ce4+ ions on the electronic conduction of Ni1−2xCexFe2O4. J. Scrp Matra. 64(8) (2011) 773-776.

38. M.I. Klinger. Two-phase polaron model of conduction in magnetite-like solids. -Phys C. J. S. S. Phys. 8 (1975) 3596-3607.

39. C. Singh, I.S.Hudiara,K. Sudheerndran, K.C. J. Rajub. Complex permittivity and complex permeability of Sr ions substituted Ba ferrite at X-band. J. Mag. Mag. Mat. 320 (2008) 1657–1665.

40. S. M. Abbas, A. K. Dixit, A. V. R. Kumar, T. C. Goel. Electromagnetic and microwave absorption properties of Co2+–Si4+ substituted barium hexaferrites and its polymer composite. J.App. Pys. 101 (2007) 074101-074106.

41. S. Daniel. M.S. Dunn, P. Eugene. Frequency dependent dielectric behaviour of caduum and chromium - cosubstituted nickle ferrite. J. Pure. App. phy. 43 (2005) 688- 690.

42. M. Ajmal, A. Maqsood. AC conductivity, density related and magnetic properties of Ni1-xZnxFe2O4 ferrites with the variation of zinc concentration. J. Mat. Lett. 62(14) (2008) 2077-2080.

43. Y.Chen1 , L. Anton. Geiler1, C.Vittoria1 , V. Zagorodnii1, Z. Celinski2, G. Vincent. Harris1. Microstructural, magnetic and microwave properties of large area BaFe12O19 Thick Films (100micometer) deposited on SiO2/Si and Al2O3/Si Substrates. IEEE- J. Trans. Mag. 44(12) (2008) 4571 - 4578.

44. S. B. Naranga, K. Singhb. High frequency dielectric behavior of rare earth substituted Sr-M hexaferrite. J. Cerm. Proc. Res. 8(5) (2007) 347-351.

45. Z. Yang, C.S. Wang, Li XH, Zeng HX: (Zn, Ni, Ti) substituted barium ferrite particles with improved temperature coefficient of coercivity. J. Mat. Sci. Engg. B 90(1–2) (2002) 142-145.

46. S. Bindra Naranga, etal. High frequency dielectricbehavior of Rare Earth Substituted Sr-M Hexaferrite. J. Cer. Proc. Res. 8(5) (2007) 347-351

47. A. Vermaa , R.G. Mendirattaa, M.I. Alam. Dielectric properties of NiZn ferrites prepared by the citrate precursor method. J. Mat. Sci. Engg. B(60) (1999) 156-162.

48. J. Qiu, M. Gu, H. Shen. Microwave absorption properties of Al- and Cr-substituted M-type barium hexaferrite. J. Mag. Mag. Mat. 295(3) (2005) 263-268.

49. S. Bindra Naranga etal. High Frequency Dielectric Behavior of Rare Earth Substituted Sr-M Hexaferrite. J. Cer. Proc. Res. 8(5) (2007) 347-351

50. Virender Pratap Singh1, Gagan Kumar1, Pooja Dhiman1, R. K. Kotnala3, Jyoti Shah3, Khalid M. Batoo4, M. Singh. Structural, dielectric and magnetic properties of nanocrystalline BaFe12O19 hexaferrite processed via sol-gel technique. J. Adv. Mat. Lett. 5(8) (2014) 447-452.

Author' biography with Photo

Dr Anwar ul Haq did his MSc from G.C. Lahore –Pakistan in 1987. He joined

Education department as lecturer. During his service he did work in the field of electronics and computer sciences as system designer and software developer.

In 2004 he joined Mphil-PhD leading program of Higher Education Department government of Pakistan. He completed his PhD in Physics (Magnetic Materials) in 2012 from Applied Thermal Physics Labortary(ATPL-Physics Department) COMSATS Institute of Information Technology, Islamabad-Pakistan . Now he has started research work in same related areas . The presented work is his post Phd work in which he analyzed the two low temperature synthesis methods and discussed the merits and demerits as he observed during the synthesis.

ISSN 2347-3487

Novelty of the Paper

In presented paper, comparative analysis of $Ba_{1-x}Pb_xFe_{12}O_{19}$ (x=0.0 to 1.0) has discussed. The composition was synthesized by two low temperature synthesis methods. They were co-precipitation and sol-gel. Synthesis parameters were optimized before going to synthesize the composition. It has reported that hard ferrites usually attain phase purity after sintering in the range of 1000°C to 1600°C for many hours. Scientists are trying to overcome these barriers in order to save the energy, time and cost. Innovations in submitted papers are

1. To address these problems I used lead as dopant and synthesized the composition through Sol-gel and Co-precipitation methods (both are low temperature synthesis techniques).
2. Lead being low melt point and higher ionic mobility enhance the crystallization process and better control on synthesis parameters achieves better properties.
3. Both samples were sintered at 965°C for three hours.
4. 70% and 100% phase purity achieved in co-precipitation and Sol-gel methods. According to my literature survey it has not reported yet that 100% Ba-hexaferrite (x=0.0) transformed into 100% Pb-hexaferrite with a step of 0.2 through sol gel.
5. Sol-gel method also modified. Nitrates and ethylene glycol were used as basic ingredients. Simple heating on hot plate at 200°C throughout synthesis and then sintering at 965°C enable us to achieve 100% phase purity.
6. Modified Sol-gel method is simple, easy and economical. No hi-tech require so very much attractive for industrial production.
7. Structural and electrical (dc and ac) were investigated and reported.
8. All properties improved in sol-gel than co-precipitation
9. Results obtained in both methods were compared and analyzed.
10. High resistivity obtained due to lead doping is useful for smart electrical devices.
11. Dielectric constant and loss obtained are useful for smart storage devices and against radiation hazards.